Virologica Sinica 37 (2022) 695–703

Contents lists available at ScienceDirect

Virologica Sinica

journal homepage: www.keaipublishing.com/en/journals/virologica-sinica
www.virosin.org

Research Article

Comparison of viral propagation and drug response among SARS-CoV-2 VOCs using replicons capable of recapitulating virion assembly and release

Lingqian Tian [a,b], Qiuhong Liu [a,b], Rongjuan Pei [a], Yingshan Chen [a,b], Chonghui Xu [a,b], Jielin Tang [d], Hao Sun [a,b], Kunpeng Liu [a,b], Qi Yang [c], Lei Yang [a,b], Leshan Li [a,b], Yongli Zhang [a], Yuan Zhou [a], Chao Shan [a], Xue Hu [a,*], Xinwen Chen [a,e,*], Yun Wang [a,*]

[a] State Key Laboratory of Virology, Wuhan Institute of Virology, Center for Biosafety Mega-Science, Chinese Academy of Sciences, Wuhan, 430071, China
[b] University of Chinese Academy of Sciences, Beijing, 100049, China
[c] Department of Gastroenterology, Guangzhou Women and Children's Medical Center, Guangzhou, 510623, China
[d] Guangzhou Institutes of Biomedicine and Health, Chinese Academy of Sciences, Guangzhou, 510530, China
[e] Innovation Center for Pathogen Research, Guangzhou Laboratory, Guangzhou, 510320, China

ARTICLE INFO

Keywords:
SARS-CoV-2
Variants of concern (VOC)
Viral-like particle (VLP)
Replicon
Remdesivir

ABSTRACT

Several variants of concern (VOCs) have emerged since the WIV04 strain of severe acute respiratory syndrome coronavirus 2 (SARS-CoV-2) was first isolated in January 2020. Due to mutations in the spike (S) protein, these VOCs have evolved to enhance viral infectivity and immune evasion. However, whether mutations of the other viral proteins lead to altered viral propagation and drug resistance remains obscure. The replicon is a noninfectious viral surrogate capable of recapitulating certain steps of the viral life cycle. Although several SARS-CoV-2 replicons have been developed, none of them were derived from emerging VOCs and could only recapitulate viral genome replication and subgenomic RNA (sgRNA) transcription. In this study, SARS-CoV-2 replicons derived from the WIV04 strain and two VOCs (the Beta and Delta variants) were prepared by removing the *S* gene from their genomes, while other structural genes remained untouched. These replicons not only recapitulate viral genome replication and sgRNA transcription but also support the assembly and release of viral-like particles, as manifested by electron microscopic assays. Thus, the *S*-deletion replicon could recapitulate virtually all the post-entry steps of the viral life cycle and provides a versatile tool for measuring viral intracellular propagation and screening novel antiviral drugs, including inhibitors of virion assembly and release. Through the quantification of replicon RNA released into the supernatant, we demonstrate that viral intracellular propagation and drug response to remdesivir have not yet substantially changed during the evolution of SARS-CoV-2 from the WIV04 strain to the Beta and Delta VOCs.

1. Introduction

Coronaviruses belong to the *Coronaviridae* family and harbor positive-sense single-stranded RNA genomes ranging from 26 to 32 kilobases (kb) (Woo et al., 2010). For most coronaviruses, replication and transcription of viral genome and genes are mediated by a replication-transcription complex (RTC) encoded by *ORF1ab*. The core component of RTC is RNA-dependent RNA polymerase (RdRp), which is recognized as the most important target for anti-viral drug development. The rest of the viral genome contains the genes encoding structural proteins, including spike (S), envelope (E), membrane (M), nucleocapsid (N), and genus-specific accessory proteins. The S protein mediates viral entry into host cells and is the primary target of neutralization antibodies (Li, 2016). The E protein and M protein form the viral envelope structure, and the N protein constitutes the nucleocapsid. These three viral structural proteins are necessary for the efficient assembly, trafficking, and release of virus-like particles (VLPs) (Siu et al., 2008; Xu et al., 2020; Boson et al., 2021). After coronaviruses enter host cells, the RTC is directly translated from positive-sense full-length genomic RNA (+fgRNA). The RTC then catalyzes viral genome replication into a negative-sense fgRNA (−fgRNA), which subsequently serves as the template for synthesizing the nascent positive-sense viral genome. RTC also catalyzes a discontinuous transcription process and generates an array of subgenomic

* Corresponding authors.
E-mail addresses: huxue@wh.iov.cn (X. Hu), chen_xinwen@gzlab.ac.cn (X. Chen), wangyun@wh.iov.cn (Y. Wang).

https://doi.org/10.1016/j.virs.2022.06.008
Received 29 March 2022; Accepted 27 June 2022
Available online 1 July 2022

RNAs (sgRNAs), which are capped with an identical transcription regulatory sequence leader (TRS-L) derived from the viral 5′-untranslated region (5′-UTR). These sgRNAs are subsequently translated into individual viral structural and accessory proteins (Fehr and Perlman, 2015).

Coronavirus disease 2019 (COVID-19) is caused by severe acute respiratory syndrome coronavirus 2 (SARS-CoV-2) (Wu et al., 2020; Zhou et al., 2020), the third deadly coronavirus after SARS-CoV, and Middle East respiratory syndrome coronavirus (MERS-CoV), which caused severe casualties in 2003 and 2012, respectively (Cui et al., 2019). Since the WIV04 strain of SARS-CoV-2 was first isolated in January 2020 (Zhou et al., 2020), several emerging variants have been reported, including the Beta and Delta variants of concern (VOCs). Compared to the WIV04 strain, overwhelming evidence has shown that S protein mutations in VOCs result in enhanced infectivity and reduced susceptibility to neutralizing antibodies (Cele et al., 2021; Li et al., 2021; Wang et al., 2021; Wibmer et al., 2021); however, whether other mutations of VOCs lead to altered viral propagation and drug resistance to remdesivir (RDV), the first FDA-approved SARS-CoV-2 RdRp inhibitor (Gordon et al., 2020; Wang et al., 2020), remains unclear.

Replicons are viral surrogates that harbor a complete set of viral genes and are involved in viral genome replication but lack some essential structural genes, resulting in a loss of infectivity. Being replication-competent but infection-defective, replicons are widely used as a safe tool for studying viral propagation and antiviral drug screening. For many coronaviruses, including SARS-CoV and MERS-CoV, replicons have already been developed (Almazan et al., 2014).

For SARS-CoV-2, none of the reported replicons were derived from emerging VOCs. In addition, most of them were constructed by simultaneously removing the *S*, *M*, and *E* genes from the viral genome (Xia et al., 2020; Furutani et al., 2021; He et al., 2021; Kotaki et al., 2021; Nguyen et al., 2021; Wang B et al., 2021; Zhang QY et al., 2021; Zhang Y et al., 2021; Liu et al., 2022; Tanaka et al., 2022; Zhang et al., 2022). Although these replicons successfully recapitulated viral genome replication and sgRNA transcription, they failed to simulate other viral propagation steps, such as virion assembly and release, due to the absence of major viral structural genes. In this study, we prepared SARS-CoV-2 replicons for the WIV04 strain and two VOCs by removing the *S* gene from the viral genome. For the first time, we demonstrated that replicon-derived VLPs could be assembled and released into the supernatant. By quantifying the replicon RNA in the supernatant, we showed that viral intracellular propagation and drug response to RDV have not yet substantially changed during SARS-CoV-2 evolution from the WIV04 strain to the Beta and Delta VOCs.

2. Materials and methods

2.1. Viruses, cell lines, chemical reagents, and biosafety

The SARS-CoV-2 WIV04 strain (IVCAS 6.7512) (Zhou et al., 2020), the Beta VOC (IVCAS 6.7552) (Meng et al., 2021), and the Delta VOC (IVCAS 6.7585) were obtained from the Microorganisms & Viruses Culture Collection Center, Wuhan Institute of Virology, Chinese Academy of Sciences. HEK-293T cells and Vero E6 cells were maintained in Dulbecco's modified Eagle's medium (HyClone, Logan, UT, USA) supplemented with 10% or 2% fetal bovine serum (Invitrogen, Darmstadt, Germany) at 37 °C. HEK-293T cells were transfected with replicons using Lipofectamine 3000 (Invitrogen, Darmstadt, Germany) according to the manufacturer's protocols. Vero E6 cells were infected with SARS-CoV-2 at a 0.01 multiplicity of infection following standard infection protocols. RDV was purchased from Selleck (Houston, TX, USA). All experiments involving live viruses were performed in the biosafety level-3 (BSL-3) facility at Wuhan Institute of Virology, CAS.

2.2. One-step isothermal assembly of SARS-CoV-2 replicons

The viral genome, excluding the indicated viral genes, was amplified into five terminally overlapping cDNA fragments by reverse-transcription PCR (RT-PCR) using a HiScript III 1st Strand cDNA Synthesis Kit (Vazyme, Nanjing, China). The relative locations of each primer used to amplify the viral cDNA clone are diagramed in Fig. 1A. To accommodate the viral cDNA clone into a bacterial artificial chromosome (BAC), several genetic elements were introduced into a previously described BAC vector pGF (Hou et al., 2016) by using the ClonExpress Ultra One Step Cloning Kit (Vazyme). These elements (from 5′ to 3′) included a CMV promoter, a hepatitis delta virus self-cleaving ribozyme (HDVrbz), and a bovine growth hormone gene polyA signal (bGHpA). The modified BAC vector was linearized by PCR using the primer pair 5HM-R/3HM-F. Viral cDNA amplicons and the linearized BAC vector (Fig. 1A) were concentrated by precipitation in 70% ethanol supplemented with 0.3 mol/L sodium acetate. Equal molar (0.05 pmol) concentrated DNA fragments were then assembled by the NEBuilder HiFi DNA assembly kit (NEB, MA, USA) according to the manufacturer's protocols.

2.3. Preparation of replicon-derived VLPs in the supernatant

Replicon-derived VLPs were harvested following a protocol previously described (Alexander et al., 2020), with minor modifications. Briefly, approximately 3×10^7 HEK-293T cells were transfected with 90 μg of replicon plasmids. At 48 h post-transfection (hpt), viral supernatants were harvested and clarified by centrifugation at 3,000 ×*g* for 20 min at 4 °C. The resulting viral supernatants were then adjusted to a final concentration of 100 mmol/L $MgSO_4$, 50 mmol/L Tris-HCl, and 10% (v/v) polyethylene glycol-6000. After incubation for 2 h at 4 °C with gentle agitation, viral supernatants were centrifuged at 3,000 ×*g* for 20 min at 4 °C. The supernatants were then discarded, and the pellet was resuspended in 0.5 mL of 1 × TE buffer.

2.4. Transmission electron microscopy (TEM) assay

Replicon-transfected HEK-293T cells were harvested, fixed, dehydrated, embedded, and sectioned as previously described (Zhou et al., 2020). The concentrated VLPs were fixed with 1% glutaraldehyde and attached to a carbon-coated 200 mesh copper grid, followed by negative staining with 1% sodium phosphotungstic acid. All the samples were subjected to TEM with an FEI Tecnai G2 TEM (Hillsboro, OR, USA) at 200 kV.

2.5. Quantitative PCR (qPCR)

Viral RNA in the supernatant of virus-infected cells or replicon-transfected cells was extracted by TRIzol-LS reagent (Invitrogen) according to the manufacturer's protocols. The RNA concentration was measured using a NanoDrop One UV-Vis spectrophotometer. All the RNA samples were digested with DNAseI (Vazyme) to remove possible DNA contamination. Two micrograms RNA were subjected to qPCR assay using One-step qRT-PCR probe Kit or Taq Pro HS Universal Probe Master Mix (Vazyme) with primers and probes targeting *orf1ab* or *N* (China CDC 2019-nCoV *ORF1ab/N* detection kit). Sequence information of all primers and TaqMan probes used in this study are listed in Supplementary Table S1.

2.6. Half-maximal inhibitory concentration (IC_{50}) and statistical analysis

The qPCR data were analyzed using the two-tailed unpaired *t*-test. A $P < 0.05$ was considered statistically significant. The viral response to RDV was represented as the value of the half maximal inhibitory concentra-

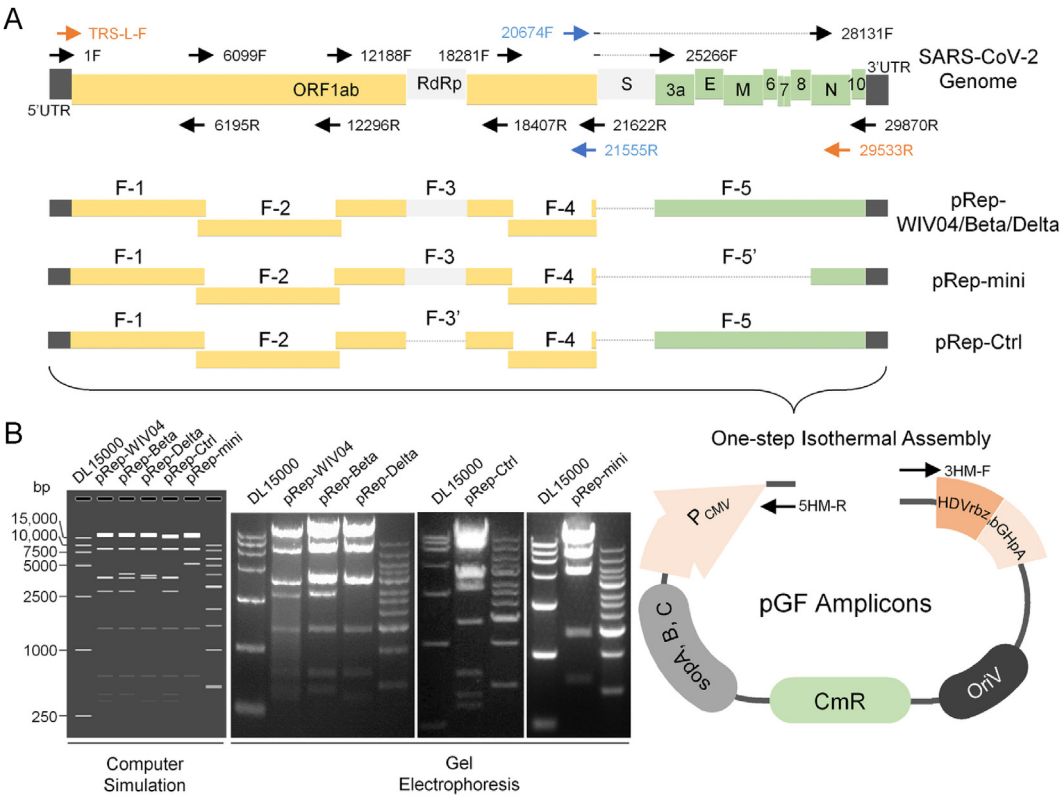

Fig. 1. Construction of the SARS-CoV-2 replicons. **A** diagram of the replicon construction. Vero E6 cells were infected with the three SARS-CoV-2 strains or variants. At 48 h post-infection, total RNA was extracted and served as a template for RT-PCR. Five primer pairs (1F/6195R, 6099F/12296R, 12188F/18407R, 18281F/21622R, and 25266F/29870R) were used to amplify the cDNA clone of the viral RNA genome and generated five fragments (F-1–F-5; F-3′ indicates F-3 without the RdRp coding sequence and F-5′ indicates F-5 without the viral sequence prior to the *N* gene). Viral cDNA amplicons were assembled into a pGF vector between a CMV promoter and an HDVrbz through a one-step isothermal assembly. The relative locations of the important primers used in this study are labeled (arrowhead). **B** Restriction assay of the replicon plasmids. The replicon plasmids were extracted from *E. coli* EPI300. Approximately 3 μg of each replicon was digested by *Nco*I. The resulting restriction fragments were separated by gel electrophoresis (1% agarose) and compared to a computer-generated gel simulation. The expected sizes of pRep-WIV04 restriction fragments were 19,076-, 8257-, 3710-, 3697-, 2793-, 1439-, 626-, 435-, 373-bp in length; for pRep-Beta, the sizes were 19,076-, 8257-, 4083-, 3697-, 2793-, 1439-, 626-, 435-bp; for pRep-Delta, the sizes were 19,112-, 8257-, 3915-, 3697-, 1439-, 626-, 373-bp; for pRep-mini, the sizes were 19,067-, 8257-, 5211-, 1439-, 626-bp; for pRep-Ctrl, the sizes were 16,679-, 8257-, 3710-, 3697-, 2793-, 1439-, 626-, 435-, 373-bp.

tion (IC_{50}), which was calculated by GraphPad Prism software with a nonlinear regression algorithm.

3. Results

3.1. SARS-CoV-2 replicons constructed by one-step isothermal assembly

The assembly products were extracted from bacterial transformants and digested by the *Nco*I endonuclease. The resulting restriction fragments were separated by gel electrophoresis and compared to a computer-generated gel simulation (Fig. 1B). A closer examination revealed that each restriction band of pRep-WIV04 appeared to be slightly lower than its counterpart of pRep-Beta and pRep-Delta (Fig. 1B). A possible explanation is that more BAC replication intermediates of higher molecular weight were present in the endonuclease digestion products of pRep-Beta and pRep-Delta than that of pRep-WIV04. The constructs with correct restriction patterns were further verified by Sanger sequencing. The mutations in the two VOC-derived replicons are summarized in Supplementary Table S2.

Replicons with a single *S* gene deletion were designated as pRep-WIV04 (derived from the WIV04 strain), pRep-Beta (derived from the Beta VOC), and pRep-Delta (derived from the Delta VOC). A mini replicon lacking *S*, *E*, *M* and all the accessory genes was designated as pRep-mini (Fig. 1A). A negative control replicon with *S* and *RdRp* dual deletion was designated as pRep-Ctrl (Fig. 1A). Both pRep-mini and pRep-Ctrl were derived from the WIV04 strain.

3.2. Replicon recapitulation of viral genome replication and sgRNA transcription

To investigate whether the *S*-deletion replicons could still produce infectious virions, supernatants from HEK-293T cells transfected with all the constructed replicons were collected and incubated with fresh Vero E6 cells. After 48 h, the infected cells were collected and subjected to qPCR assay. All the samples were below the detection threshold, indicating that the *S*-free replicons cannot produce infectious virions.

Since the replicon vector is controlled by a CMV promoter, +fgRNAs can be produced by either viral RdRp or cellular RNA polymerase II. In contrast, the −fgRNAs are solely produced by viral RdRp and serve as the template for RdRp-dependent viral genome replication. To explore whether the assembled replicons could recapitulate viral genome replication of their parental viruses, we attempted to detect replicon-derived −fgRNAs. HEK-293T cells were transfected with replicons, and Vero E6 cells were infected with their parental viruses. Total RNA was extracted as the template for reverse transcription. An oligonucleotide hybridized with the negative-sense *ORF1ab* (20674F, diagramed in Fig. 1A) was used as a gene-specific primer to prime reverse transcription, thus ensuring that only RdRp-transcribed −fgRNA could be converted into cDNA. An anti-sense primer (21555R, diagramed in Fig. 1A) was paired with 20674F to amplify a fragment of fgRNA-derived cDNA. RT-PCR amplicons from pRep-WIV04-, pRep-Beta-, pRep-Delta-, and pRep-mini-transfected cells or their parental virus-infected cells were 882 bp in length, whereas no

specific amplicon could be amplified from pRep-Ctrl (Fig. 2A). The amplicons were further verified by Sanger sequencing, indicating that the pRep-WIV04, pRep-Beta, pRep-Delta, and pRep-mini could successfully recapitulate the viral genome replication of their parental viruses.

As they are capped with TRS-L, sgRNAs are the characteristic transcriptional products of SARS-CoV-2. To test whether the replicons could recapitulate the transcription step of their parental viruses, we attempted to detect the replicon-derived sgRNA. HEK-293T cells were transfected with replicons, and Vero E6 cells were infected with their parental viruses. A sense primer (TRS-L-F) was designed to anneal with the TRS-L region of SARS-CoV-2, and an anti-sense primer was designed to anneal with the 3′-end of the *N* gene (29533R). The PCR extension time was adjusted according to the *N* gene length, thus ensuring that only sgRNAs encoding N protein could be specifically amplified. RT-PCR amplicons from replicon-transfected cells and parental virus-infected cells were all about 1.3 kb in length, whereas no specific amplicon could be detected in pRep-Ctrl-transfected cells (Fig. 2B). Sequence analysis of the sequenced amplicons revealed that all the replicon-derived sgRNAs contained a common TRS-L sequence at their 5′ ends, followed by the *N* gene sequences (Fig. 2C), indicating that the pRep-WIV04, pRep-Beta, pRep-Delta, and pRep-mini could successfully recapitulate the sgRNA transcription step of their parental viruses.

3.3. Replicon recapitulation of virion assembly and release

To the best of our knowledge, all the currently studies reporting SARS-CoV-2 replicons did not address whether they could recapitulate virion assembly and release, the final steps of the viral life cycle. Two WIV04-derived replicons, pRep-WIV04 and pRep-mini, were transfected into HEK-293T cells. At 24 hpt, viral contents were subjected to a TEM assay. In pRep-WIV04-transfected cells, spherical particles, which were approximately 100 nm in diameter and with electron-dense materials, were present in the lumen of small vesicles beneath the cell membrane (Fig. 3A). The morphological and spatial patterns of the spherical particles were in consistence with those of SARS-CoV-2 virions (Eymieux et al., 2021a, 2021b), and implied that they were replicon-derived VLPs. In contrast, no such particles could be found in the cells transfected with pRep-mini (Fig. 3B), indicating that the presence of *E* and *M* in the replicon was necessary for VLP formation and that pRep-WIV04 could recapitulate virion assembly of its parental virus. Actually, this conclusion is in accordance with a previous report that M and E play an essential role in VLP formation (Xu et al., 2020). To investigate whether replicon-derived VLPs could be released, the viral contents in the supernatant of pRep-WIV04-transfected cells were concentrated and subjected to TEM. Negatively strained VLPs were readily found (Fig. 3C), implying that pRep-WIV04 could also support the recapitulation of virion release of its parental virus.

Taken together, our evidence suggests that the *S*-deletion replicon could serve as a versatile tool to recapitulate virtually all the post-entry steps of the SARS-CoV-2 life cycle, including viral genome replication, sgRNA transcription, virion assembly, and release.

3.4. Comparison of viral intracellular propagation among SARS-CoV-2 variants

Since we demonstrated that the VLP derived from the *S*-deletion replicon could be released into the supernatant, we therefore attempted

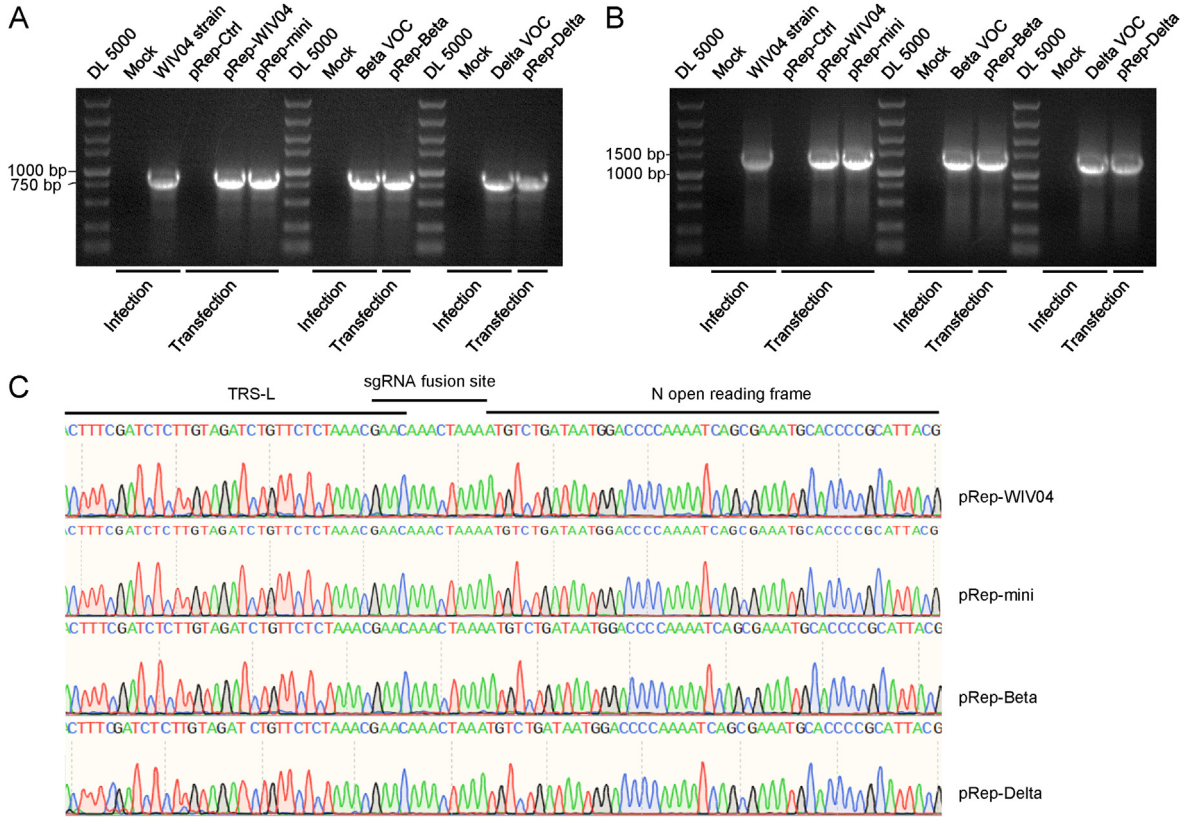

Fig. 2. The replicon recapitulates viral genome replication and sgRNA transcription. Vero E6 cells were infected with the three SARS-CoV-2 strains or variants, and HEK-293T cells were transfected with the indicated replicon plasmids. Total RNA was extracted from both the infected and transfected cells and served as the template for RT-PCR. To detect −fgRNA, reverse transcription was primed with 20674F, and the resulting cDNA was amplified with the primer pair 20674F/21555R (**A**). To detect the sgRNA encoding the N protein, reverse transcription was primed with oligo(dT), and RT-PCR amplified the resulting cDNA with the primer pair TRS-L-F/29533R (**B**). The abovementioned RT-PCR amplicons were subjected to Sanger sequencing, and a common TRS-L motif and a fusion site were identified in all the sequenced samples (**C**).

to measure viral propagation by quantifying replicon RNA packed in the released VLP.

Replicons were transfected into HEK-293T cells. At 6, 12, 24, 48, and 72 hpt, the supernatants were collected, and total RNA was extracted and subjected to qPCR using a China CDC 2019-nCoV *ORF1ab* detection kit. Extracellular replicon RNAs (ERR) derived from pRep-Ctrl and pRep-mini remained below the detection threshold at all time points (Fig. 4A). This phenotype demonstrated that although replicon RNA derived from pRep-mini could be detected intracellularly as shown in Fig. 2, it failed to be released into the supernatant. As a contrast, ERR derived from pRep-WIV04, pRep-Beta, and pRep-Delta, were readily detected and simultaneously increased and decreased with similar kinetics without significant differences (Fig. 4A). Replicon RNA thus appears to be packed in and released with VLP as ERR, since VLP-deficient pRep-mini failed to generate detectable ERR. In addition, the presence of ERR suggested that VLPs derived from *S*-deletion replicons also contained N protein, as packaging of viral RNA into VLP was dependent on the N protein (Chen et al., 2021).

In parallel, intracellular replicon RNA was measured. To exclude the positive-sense replicon RNA that could be transcribed by cellular RNA polymerase II, total intracellular RNA was first reverse-transcribed by 20674F. The resulting −fgRNA-derived cDNA was quantified by qPCR using the China CDC 2019-nCoV *N* detection kit. Consistent with replicon RNA in the supernatant, the intracellular −fgRNA derived from pRep-WIV04, pRep-Beta, and pRep-Delta showed similar propagation kinetics without significant differences (Fig. 4B). Taken together, these results indicate that the WIV04 strain and the two VOCs share virtually the same propagation kinetics during the post-entry steps, which was demonstrated by both quantifications of the extracellular and intracellular replicon RNA.

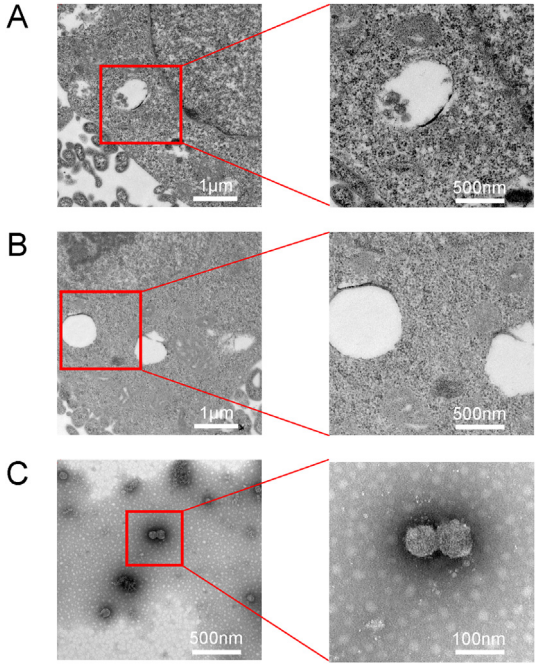

Fig. 3. TEM assay of replicon-derived VLPs. **A**, **B** VLP assembly in replicon-transfected cells. HEK-293T cells were transfected with pRep-WIV04 (**A**) or pRep-mini (**B**). At 24 h post-transfection, the cells were subjected to TEM assay. **C** VLP present in the supernatant. The supernatant of pRep-WIV04-transfected cells was collected, and the viral contents were negatively stained and subjected to TEM assay. The boxed regions are shown at higher magnification in the right panels.

3.5. Comparison of viral response to the RDV treatment among SARS-CoV-2 variants

To assess the viral drug response, serially diluted RDV was applied to HEK-293T cells transfected with pRep-WIV04, pRep-Beta, and pRep-Delta. At 24 h following RDV treatment, ERR was extracted from the supernatant and quantified by qPCR using a China CDC 2019-nCoV *ORF1ab* detection kit. For all three replicons, the copy number of ERR declined with increasing RDV concentration. There were no significant differences among the three replicons concerning ERR reduction level at all the tested RDV concentrations (Fig. 5A), suggesting that the viral response to RDV treatment has not yet substantially changed during the evolution of SARS-CoV-2 from the WIV04 strain to the Beta and the Delta VOCs.

In parallel, Vero E6 cells were infected with their parental viruses. At 24 h following RDV treatment, extracellular RNA was extracted from viral supernatants and subjected to a similar qPCR assay to quantify viral genomes packed in the secreted virions. Based on the reduction in viral genome copy number, the IC_{50} value of RDV against WIV04 strain was 0.5011 μmol/L on average and that of the Beta and Delta VOCs was 0.5596 μmol/L and 0.4129 μmol/L (Fig. 5B), respectively. Therefore, evidence from infectious viruses is consistent with that from replicons, and both support the conclusion that RDV is still an effective antiviral drug for the two VOCs.

4. Discussion

The viral genome of SARS-CoV-2 is nearly 30 kb in length and is one of the largest RNA viral genomes. To construct replicons or infectious clones for SARS-CoV-2, both *in vivo* and *in vitro* assembly methods were attempted. For the *in vivo* approach, transformation-associated recombineering (TAR) was employed to assemble the first SARS-CoV-2 infectious clone (Thi Nhu Thao et al., 2020), as well as various types of replicons (Ricardo-Lax et al., 2021; Wang B et al., 2021). The SARS-CoV-2 cDNA amplicons were transformed into yeast cells to assemble into a replicon by homologous recombination. The resulting assembly products were then extracted and retransformed into *E. coli* for high-efficiency multiplication before the replicon construct could be used. For the *in vitro* approach, one popular method is to digest SARS-CoV-2 cDNA amplicons with either regular restriction enzymes (Jin et al., 2021; Nguyen et al., 2021; Zhang QY et al., 2021) or type IIS restriction enzymes (Xia et al., 2020; Xie et al., 2020; Kotaki et al., 2021; Xie et al., 2021; Zhang et al., 2021; Liu et al., 2022). The resulting restriction fragments were then ligated into a full-length replicon using T_4 DNA ligase. Another convenient method is based on circular polymerase extension reaction (CPER) (Edmonds et al., 2013). SARS-CoV-2 genome was reverse-transcribed and amplified into several overlapping cDNA amplicons. These viral amplicons, together with a linker sequence containing CMV promoter, HDVrbz, and polyA signal were extended into circular form by DNA polymerase (Amarilla et al., 2021; Torii et al., 2021; Tanaka et al., 2022). However, the resulting circular DNA could not propagate and be preserved in *E. coli* due to lack of plasmid replication origin.

In contrast to multistep methods that were previously attempted for the preparation of SARS-CoV-2 replicons, we developed a one-step method to assemble SARS-CoV-2 cDNA amplicons into a full-length replicon using the NEBuilder HiFi DNA assembly kit. Compared to previously reported multistep assembly methods, the one-step method was apparently more convenient and the efficiency of legitimate assembly was up to 40%–60% in this study. Compared to CPER-based method, the replicons constructed in this study could be amplified and preserved in *E. coli* as plasmids, providing convenience in preserving and exchanging research materials.

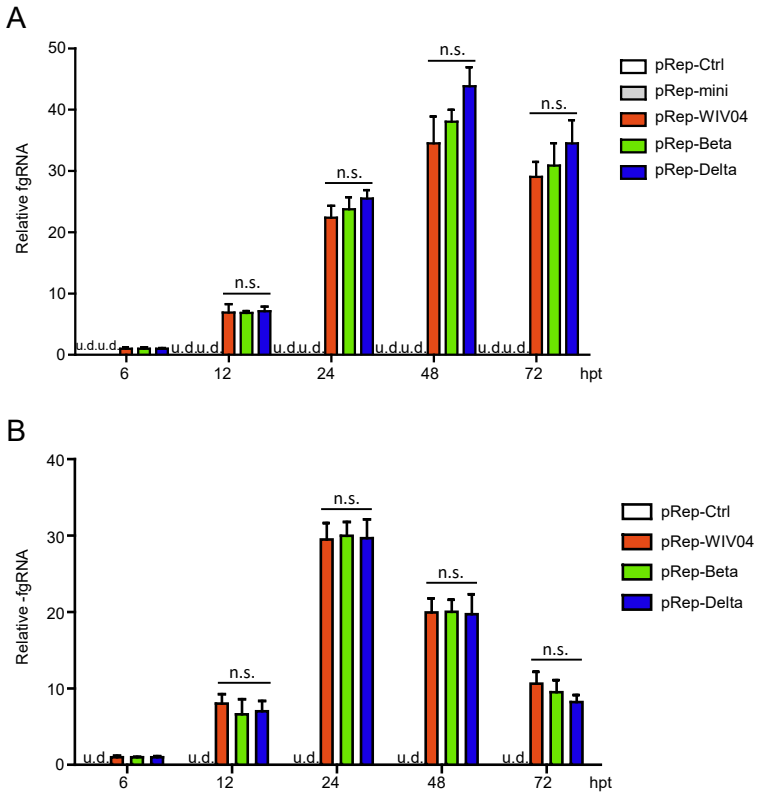

Fig. 4. Comparison of viral intracellular propagation among SARS-CoV-2 variants. **A** Quantification of replicon RNA in the supernatant. HEK-293T cells were transfected with the indicated replicons. At 6, 12, 24, 48, and 72 h post-transfection (hpt), ERR in the supernatants was quantified by qPCR. The relative increase in individual replicon RNA is presented as the ratio of fgRNA copy number at the indicated time points to that at 6 hpt. **B** Quantification of intracellular replicon RNA. HEK-293T cells were transfected with the indicated replicons. At 6, 12, 24, 48, and 72 hpt, total RNA was extracted from transfected cells and was reverse-transcribed using the gene-specific primer 20674F. The resulting −fgRNA-derived cDNA was then quantified by qPCR. The relative increase in individual −fgRNA is presented in a way similar to that of (**A**). All experiments were performed in triplicate. The data points indicate the averages of triplicate experiments. The error bars indicate the standard derivation from the mean. n.s., not significant; u.d., undetectable.

Different types of tools have been developed to recapitulate different steps of the viral life cycle. Pseudotyped viruses enveloped with the S protein were frequently used to recapitulate viral cell entry. Replicons with *S*, *M*, *E* triple structural gene deletion could be used to recapitulate viral genome replication and sgRNA transcription. However, whether virion assembly and release, the final steps of the viral life cycle could be recapitulated by replicons remained undetected. Although other groups have developed similar replicons with a single *S*-deletion (Jin et al., 2021; Ricardo-Lax et al., 2021; Malicoat et al., 2022), none of them tested whether their replicons supported the formation and release of VLP without *trans*-complementation with S or VSV-G (Ricardo-Lax et al., 2021; Malicoat et al., 2022). In this study, we demonstrated for the first time that the *S*-deletion replicon could recapitulate all the post-entry steps of the SARS-CoV-2 life cycle, particularly virion assembly and release.

The virions released to the supernatant are the final product of SARS-CoV-2 propagation, and the level of which can be influenced by antiviral drugs that target any viral propagation step, including cell entry, viral genome replication and sgRNA transcription, and virion assembly and release. Thus, quantifying ERR packed in the released VLP would be an appropriate way to measure the overall level of viral propagation and antiviral efficacy. To the best of our knowledge, all the currently reported SARS-CoV-2 replicons were engineered with a reporter gene that encoded a fluorescent or luminescent protein for viral detection or quantification. Unlike the viral RNA released to the supernatant, which could reflect the overall viral propagation, expression of the reporter gene could only indicate sgRNA transcription, one of the post-entry steps of viral propagation. Accordingly, replicons dependent on reporter gene expression could be used only to screen antiviral drugs targeting viral genome replication and sgRNA transcription but not virion assembly and release. Although most currently available anti-SARS-CoV-2 drugs, such as the RdRp inhibitor RDV and the Mpro inhibitor Paxlovid (Owen et al., 2021), target the viral genome replication and sgRNA transcription step, increasing efforts have been made to identify novel drugs that target virion assembly and release (Bhowmik et al., 2020; Dey et al., 2020; Das et al., 2021). The significance of developing a SARS-CoV-2 replicon supporting VLP assembly and release is to provide a versatile tool to screen novel antiviral drugs, including inhibitors of virion assembly and release. However, we must acknowledge that traditional replicons not supporting VLP formation are still valuable tools as they can provide a fail-safe option in common laboratory settings.

An increasing number of SARS-CoV-2 variants have emerged since the outbreak of COVID-19. Compared to the WIV04 strain and other variants, including the Beta VOC, the Delta VOC possesses a much higher viral load, which correlates with its enhanced transmission efficiency (Teyssou et al., 2021). Although the S protein mutation P681R was demonstrated to be associated with enhanced viral pathogenicity of the Delta VOC (Saito et al., 2021), whether the S mutation is fully responsible for such a high viral load remains obscure. Using the *S*-deletion replicons prepared in this study, we found that all three replicons possessed similar replicon propagation kinetics. Since the replicon could recapitulate all post-entry steps of its parental virus, the only factor contributing to the high viral load of the Delta VOC is the cell entry step.

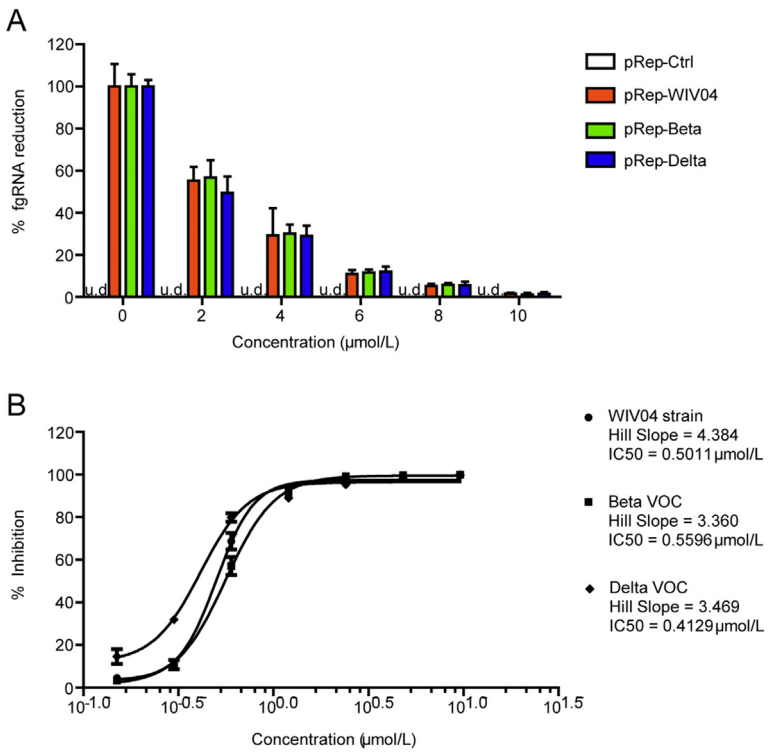

Fig. 5. Comparison of viral response to RDV treatment among SARS-CoV-2 variants. **A** Evaluation of the drug response using viral replicons. HEK-293T cells were transfected with indicated replicons. RDV was added to the culture medium at 6 h post-transfection. After 24 h of drug treatment, ERR was extracted from the supernatant and quantified by qPCR. The replicon response to RDV treatment is presented as the ratio of fgRNA copy number at the indicated RDV concentrations to that of the no drug treatment control. **B** Evaluation of drug response using infectious viruses. Vero E6 cells were infected with the three SARS-CoV-2 strains or variants at an MOI of 0.02. The infected cells were incubated with culture medium containing RDV at the indicated concentrations for 24 h. The viral yield in the cell supernatant was then quantified by qPCR. The Y-axis represents the mean % reduction in viral genome copy number. All experiments were performed in triplicate. The data points indicate the averages of triplicate experiments. The error bars indicate the standard derivation from the mean. The IC_{50} values were calculated by GraphPad PRISM. u.d., undetectable.

There is no doubt that more SARS-CoV-2 variants with enhanced infectivity may emerge as the COVID-19 pandemic continues. The replicons supporting VLP assembly and release could provide a safe and versatile platform to measure viral propagation and screen antiviral drugs for current and future emerging SARS-CoV-2 variants.

5. Conclusions

In this study, we developed an efficient assembly method and successfully constructed a SARS-CoV-2 replicon that only removed the *S* gene. For the first time, we demonstrated that the S-deletion replicon could recapitulate all the post-entry steps of the SARS-CoV-2 life cycle, especially the assembly and release of virions. This makes it possible to provide a safe and versatile platform to measure viral propagation and screen antiviral drugs for current and future emerging SARS-CoV-2 variants. Subsequently, we used the S-deletion replicon to demonstrate that viral intracellular propagation and drug response to remdesivir had not yet substantially changed during the evolution of SARS-CoV-2 from the WIV04 strain to Beta and Delta VOCs.

Data availability

All the data generated during the current study are included in the manuscript.

Ethics statement

This study does not contain any studies with human or animal subjects performed by any of the authors.

Author contributions

Lingqian Tian: data curation, investigation, methodology, Qiuhong Liu: data curation, investigation, methodology. Rongjuan Pei: formal analysis, investigation, supervision. Yingshan Chen: investigation, methodology. Chonghui Xu: methodology. Jielin Tang: funding acquisition, methodology. Hao Sun: investigation, methodology. Kunpeng Liu: validation. Qi Yang: formal analysis, funding acquisition. Lei Yang: methodology. Leshan Li: methodology. Yongli Zhang: investigation, methodology. Yuan Zhou: project administration, resources. Chao Shan: formal analysis, supervision. Xue Hu: data curation, formal analysis, investigation, validation. Xinwen Chen: conceptualization, funding acquisition, Writing - review & editing. Yun Wang: conceptualization, formal analysis, funding acquisition, investigation, supervision, writing - original draft.

Conflict of interest

The authors declare that they have no conflict of interest.

Acknowledgment

We are grateful to Mr. Tao Du, Mr. Hao Tang, and Mr. Jun Liu of the BSL-3 laboratory at the Wuhan Institute of Virology, CAS, for their technical assistance. We also appreciate the kind help from Dr. Changwen Ke of Guangdong Provincial Center for Disease Control and Prevention. This work was supported by grants from the National Key Research and Development Project of China (2020YFC0845900) and the China Postdoctoral Science Foundation (2020T130021ZX, 2021M693198).

Appendix A. Supplementary data

Supplementary data to this article can be found online at https://doi.org/10.1016/j.virs.2022.06.008.

References

Alexander, M.R., Rootes, C.L., van Vuren, P.J., Stewart, C.R., 2020. Concentration of infectious SARS-CoV-2 by polyethylene glycol precipitation. J. Virol. Methods 286, 113977.

Almazan, F., Sola, I., Zuniga, S., Marquez-Jurado, S., Morales, L., Becares, M., Enjuanes, L., 2014. Coronavirus reverse genetic systems: Infectious clones and replicons. Virus Res. 189, 262–270.

Amarilla, A.A., Sng, J.D.J., Parry, R., Deerain, J.M., Potter, J.R., Setoh, Y.X., Rawle, D.J., Le, T.T., Modhiran, N., Wang, X., Peng, N.Y.G., Torres, F.J., Pyke, A., Harrison, J.J., Freney, M.E., Liang, B., McMillan, C.L.D., Cheung, S.T.M., Guevara, D., Hardy, J.M., Bettington, M., Muller, D.A., Coulibaly, F., Moore, F., Hall, R.A., Young, P.R., Mackenzie, J.M., Hobson-Peters, J., Suhrbier, A., Watterson, D., Khromykh, A.A., 2021. A versatile reverse genetics platform for SARS-CoV-2 and other positive-strand RNA viruses. Nat. Commun. 12, 3431.

Bhowmik, D., Nandi, R., Jagadeesan, R., Kumar, N., Prakash, A., Kumar, D., 2020. Identification of potential inhibitors against SARS-CoV-2 by targeting proteins responsible for envelope formation and virion assembly using docking based virtual screening, and pharmacokinetics approaches. Infect. Genet. Evol. 84, 104451.

Boson, B., Legros, V., Zhou, B., Siret, E., Mathieu, C., Cosset, F.L., Lavillette, D., Denolly, S., 2021. The SARS-CoV-2 envelope and membrane proteins modulate maturation and retention of the spike protein, allowing assembly of virus-like particles. J. Biol. Chem. 296, 100111.

Cele, S., Gazy, I., Jackson, L., Hwa, S.H., Tegally, H., Lustig, G., Giandhari, J., Pillay, S., Wilkinson, E., Naidoo, Y., Karim, F., Ganga, Y., Khan, K., Bernstein, M., Balazs, A.B., Gosnell, B.I., Hanekom, W., Moosa, M.S., , Network for Genomic Surveillance in South A, Team, C.-K., Lessells, R.J., de Oliveira, T., Sigal, A., 2021. Escape of SARS-CoV-2 501Y.V2 from neutralization by convalescent plasma. Nature 593, 142–146.

Chen, M., Yan, C., Qin, F., Zheng, L., Zhang, X.E., 2021. The intraviral protein-protein interaction of SARS-CoV-2 reveals the key role of N protein in virus-like particle assembly. Int. J. Biol. Sci. 17, 3889–3897.

Cui, J., Li, F., Shi, Z.L., 2019. Origin and evolution of pathogenic coronaviruses. Nat. Rev. Microbiol. 17, 181–192.

Das, G., Das, T., Chowdhury, N., Chatterjee, D., Bagchi, A., Ghosh, Z., 2021. Repurposed drugs and nutraceuticals targeting envelope protein: A possible therapeutic strategy against COVID-19. Genomics 113, 1129–1140.

Dey, D., Borkotoky, S., Banerjee, M., 2020. In silico identification of Tretinoin as a SARS-CoV-2 envelope (E) protein ion channel inhibitor. Comput. Biol. Med. 127, 104063.

Edmonds, J., van Grinsven, E., Prow, N., Bosco-Lauth, A., Brault, A.C., Bowen, R.A., Hall, R.A., Khromykh, A.A., 2013. A novel bacterium-free method for generation of flavivirus infectious DNA by circular polymerase extension reaction allows accurate recapitulation of viral heterogeneity. J. Virol. 87, 2367–2372.

Eymieux, S., Rouille, Y., Terrier, O., Seron, K., Blanchard, E., Rosa-Calatrava, M., Dubuisson, J., Belouzard, S., Roingeard, P., 2021a. Ultrastructural modifications induced by SARS-CoV-2 in Vero cells: A kinetic analysis of viral factory formation, viral particle morphogenesis and virion release. Cell. Mol. Life Sci. 78, 3565–3576.

Eymieux, S., Uzbekov, R., Rouille, Y., Blanchard, E., Hourioux, C., Dubuisson, J., Belouzard, S., Roingeard, P., 2021b. Secretory vesicles are the principal means of SARS-CoV-2 egress. Cells 10, 2047.

Fehr, A.R., Perlman, S., 2015. Coronaviruses: An overview of their replication and pathogenesis. Methods Mol. Biol. 1282, 1–23.

Furutani, Y., Toguchi, M., Higuchi, S., Yanaka, K., Gailhouste, L., Qin, X.Y., Masaki, T., Ochi, S., Matsuura, T., 2021. Establishment of a rapid detection system for ISG20-dependent SARS-CoV-2 subreplicon RNA degradation induced by interferon-alpha. Int. J. Mol. Sci. 22, 11641.

Gordon, C.J., Tchesnokov, E.P., Woolner, E., Perry, J.K., Feng, J.Y., Porter, D.P., Gotte, M., 2020. Remdesivir is a direct-acting antiviral that inhibits RNA-dependent RNA polymerase from severe acute respiratory syndrome coronavirus 2 with high potency. J. Biol. Chem. 295, 6785–6797.

He, X., Quan, S., Xu, M., Rodriguez, S., Goh, S.L., Wei, J., Fridman, A., Koeplinger, K.A., Carroll, S.S., Grobler, J.A., Espeseth, A.S., Olsen, D.B., Hazuda, D.J., Wang, D., 2021. Generation of SARS-CoV-2 reporter replicon for high-throughput antiviral screening and testing. Proc. Natl. Acad. Sci. U. S. A. 118, e2025866118.

Hou, Z., Zhou, Z., Wang, Z., Xiao, G., 2016. Assembly of long DNA sequences using a new synthetic Escherichia coli-yeast shuttle vector. Virol. Sin. 31, 160–167.

Jin, Y.Y., Lin, H., Cao, L., Wu, W.C., Ji, Y., Du, L., Jiang, Y., Xie, Y., Tong, K., Xing, F., Zheng, F., Shi, M., Pan, J.A., Peng, X., Guo, D., 2021. A convenient and biosafe replicon with accessory genes of SARS-CoV-2 and its potential application in antiviral drug discovery. Virol. Sin. 36, 913–923.

Kotaki, T., Xie, X., Shi, P.Y., Kameoka, M., 2021. A PCR amplicon-based SARS-CoV-2 replicon for antiviral evaluation. Sci. Rep. 11, 2229.

Li, F., 2016. Structure, function, and evolution of coronavirus spike proteins. Annu Rev Virol 3, 237–261.

Li, Q., Nie, J., Wu, J., Zhang, L., Ding, R., Wang, H., Zhang, Y., Li, T., Liu, S., Zhang, M., Zhao, C., Liu, H., Nie, L., Qin, H., Wang, M., Lu, Q., Li, X., Liu, J., Liang, H., Shi, Y., Shen, Y., Xie, L., Zhang, L., Qu, X., Xu, W., Huang, W., Wang, Y., 2021. SARS-CoV-2 501Y.V2 variants lack higher infectivity but do have immune escape. Cell 184, 2362–2371 e2369.

Liu, S., Chou, C.K., Wu, W.W., Luan, B., Wang, T.T., 2022. Stable cell clones harboring self-replicating SARS-CoV-2 RNAs for drug screen. J. Virol. 96, e0221621.

Malicoat, J., Manivasagam, S., Zuniga, S., Sola, I., McCabe, D., Rong, L., Perlman, S., Enjuanes, L., Manicassamy, B., 2022. Development of a single-cycle infectious SARS-CoV-2 virus replicon particle system for use in biosafety level 2 laboratories. J. Virol. 96, e0183721.

Meng, J., Mei, S., Chen, L., Wu, C., Fang, S., Peng, B., Kong, D., Zhang, X., Xiong, L., Huang, Y., Chen, Q., Zhang, R., He, Y., 2021. In: China CDC Weekly, 3, pp. 218–220.

Nguyen, H.T., Falzarano, D., Gerdts, V., Liu, Q., 2021. Construction of a noninfectious SARS-CoV-2 replicon for antiviral-drug testing and gene function studies. J. Virol. 95, e0068721.

Owen, D.R., Allerton, C.M.N., Anderson, A.S., Aschenbrenner, L., Avery, M., Berritt, S., Boras, B., Cardin, R.D., Carlo, A., Coffman, K.J., Dantonio, A., Di, L., Eng, H., Ferre, R., Gajiwala, K.S., Gibson, S.A., Greasley, S.E., Hurst, B.L., Kadar, E.P., Kalgutkar, A.S., Lee, J.C., Lee, J., Liu, W., Mason, S.W., Noell, S., Novak, J.J., Obach, R.S., Ogilvie, K., Patel, N.C., Pettersson, M., Rai, D.K., Reese, M.R., Sammons, M.F., Sathish, J.G., Singh, R.S.P., Steppan, C.M., Stewart, A.E., Tuttle, J.B., Updyke, L., Verhoest, P.R., Wei, L., Yang, Q., Zhu, Y., 2021. An oral SARS-CoV-2 M(pro) inhibitor clinical candidate for the treatment of COVID-19. Science 374, 1586–1593.

Ricardo-Lax, I., Luna, J.M., Thao, T.T.N., Le Pen, J., Yu, Y., Hoffmann, H.H., Schneider, W.M., Razooky, B.S., Fernandez-Martinez, J., Schmidt, F., Weisblum, Y., Trueb, B.S., Berenguer Veiga, I., Schmied, K., Ebert, N., Michailidis, E., Peace, A., Sanchez-Rivera, F.J., Lowe, S.W., Rout, M.P., Hatziioannou, T., Bieniasz, P.D., Poirier, J.T., MacDonald, M.R., Thiel, V., Rice, C.M., 2021. Replication and single-cycle delivery of SARS-CoV-2 replicons. Science 374, 1099–1106.

Saito, A., Irie, T., Suzuki, R., Maemura, T., Nasser, H., Uriu, K., Kosugi, Y., Shirakawa, K., Sadamasu, K., Kimura, I., Ito, J., Wu, J., Iwatsuki-Horimoto, K., Ito, M., Yamayoshi, S., Loeber, S., Tsuda, M., Wang, L., Ozono, S., Butlertanaka, E.P., Tanaka, Y.L., Shimizu, R., Shimizu, K., Yoshimatsu, K., Kawabata, R., Sakaguchi, T., Tokunaga, K., Yoshida, I., Asakura, H., Nagashima, M., Kazuma, Y., Nomura, R., Horisawa, Y., Yoshimura, K., Takaori-Kondo, A., Imai, M., , Genotype to Phenotype Japan C, Tanaka, S., Nakagawa, S., Ikeda, T., Fukuhara, T., Kawaoka, Y., Sato, K., 2021. Enhanced fusogenicity and pathogenicity of SARS-CoV-2 Delta P681R mutation. Nature 602, 300–306.

Siu, Y.L., Teoh, K.T., Lo, J., Chan, C.M., Kien, F., Escriou, N., Tsao, S.W., Nicholls, J.M., Altmeyer, R., Peiris, J.S., Bruzzone, R., Nal, B., 2008. The M, E, and N structural proteins of the severe acute respiratory syndrome coronavirus are required for efficient assembly, trafficking, and release of virus-like particles. J. Virol. 82, 11318–11330.

Tanaka, T., Saito, A., Suzuki, T., Miyamoto, Y., Takayama, K., Okamoto, T., Moriishi, K., 2022. Establishment of a stable SARS-CoV-2 replicon system for application in high-throughput screening. Antivir. Res. 199, 105268.

Teyssou, E., Delagreverie, H., Visseaux, B., Lambert-Niclot, S., Brichler, S., Ferre, V., Marot, S., Jary, A., Todesco, E., Schnuriger, A., Ghidaoui, E., Abdi, B., Akhavan, S., Houhou-Fidouh, N., Charpentier, C., Morand-Joubert, L., Boutolleau, D., Descamps, D., Calvez, V., Marcelin, A.G., Soulie, C., 2021. The Delta SARS-CoV-2 variant has a higher viral load than the Beta and the historical variants in nasopharyngeal samples from newly diagnosed COVID-19 patients. J. Infect. 83, e1–e3.

Thi Nhu Thao, T., Labroussaa, F., Ebert, N., V'Kovski, P., Stalder, H., Portmann, J., Kelly, J., Steiner, S., Holwerda, M., Kratzel, A., Gultom, M., Schmied, K., Laloli, L., Husser, L., Wider, M., Pfaender, S., Hirt, D., Cippa, V., Crespo-Pomar, S., Schroder, S., Muth, D., Niemeyer, D., Corman, V.M., Muller, M.A., Drosten, C., Dijkman, R., Jores, J., Thiel, V., 2020. Rapid reconstruction of SARS-CoV-2 using a synthetic genomics platform. Nature 582, 561–565.

Torii, S., Ono, C., Suzuki, R., Morioka, Y., Anzai, I., Fauzyah, Y., Maeda, Y., Kamitani, W., Fukuhara, T., Matsuura, Y., 2021. Establishment of a reverse genetics system for SARS-CoV-2 using circular polymerase extension reaction. Cell Rep. 35, 109014.

Wang, B., Zhang, C., Lei, X., Ren, L., Zhao, Z., Wang, J., Huang, H., 2021a. Construction of non-infectious SARS-CoV-2 replicons and their application in drug evaluation. Virol. Sin. 36, 890–900.

Wang, M., Cao, R., Zhang, L., Yang, X., Liu, J., Xu, M., Shi, Z., Hu, Z., Zhong, W., Xiao, G., 2020. Remdesivir and chloroquine effectively inhibit the recently emerged novel coronavirus (2019-nCoV) in vitro. Cell Res. 30, 269–271.

Wang, P., Nair, M.S., Liu, L., Iketani, S., Luo, Y., Guo, Y., Wang, M., Yu, J., Zhang, B., Kwong, P.D., Graham, B.S., Mascola, J.R., Chang, J.Y., Yin, M.T., Sobieszczyk, M., Kyratsous, C.A., Shapiro, L., Sheng, Z., Huang, Y., Ho, D.D., 2021b. Antibody resistance of SARS-CoV-2 variants B.1.351 and B.1.1.7. Nature 593, 130–135.

Wibmer, C.K., Ayres, F., Hermanus, T., Madzivhandila, M., Kgagudi, P., Oosthuysen, B., Lambson, B.E., de Oliveira, T., Vermeulen, M., van der Berg, K., Rossouw, T., Boswell, M., Ueckermann, V., Meiring, S., von Gottberg, A., Cohen, C., Morris, L., Bhiman, J.N., Moore, P.L., 2021. SARS-CoV-2 501Y.V2 escapes neutralization by South African COVID-19 donor plasma. Nat. Med. 27, 622–625.

Woo, P.C., Huang, Y., Lau, S.K., Yuen, K.Y., 2010. Coronavirus genomics and bioinformatics analysis. Viruses 2, 1804–1820.
Wu, F., Zhao, S., Yu, B., Chen, Y.M., Wang, W., Song, Z.G., Hu, Y., Tao, Z.W., Tian, J.H., Pei, Y.Y., Yuan, M.L., Zhang, Y.L., Dai, F.H., Liu, Y., Wang, Q.M., Zheng, J.J., Xu, L., Holmes, E.C., Zhang, Y.Z., 2020. A new coronavirus associated with human respiratory disease in China. Nature 579, 265–269.
Xia, H., Cao, Z., Xie, X., Zhang, X., Chen, J.Y., Wang, H., Menachery, V.D., Rajsbaum, R., Shi, P.Y., 2020. Evasion of type I interferon by SARS-CoV-2. Cell Rep. 33, 108234.
Xie, X., Lokugamage, K.G., Zhang, X., Vu, M.N., Muruato, A.E., Menachery, V.D., Shi, P.Y., 2021. Engineering SARS-CoV-2 using a reverse genetic system. Nat. Protoc. 16, 1761–1784.
Xie, X., Muruato, A., Lokugamage, K.G., Narayanan, K., Zhang, X., Zou, J., Liu, J., Schindewolf, C., Bopp, N.E., Aguilar, P.V., Plante, K.S., Weaver, S.C., Makino, S., LeDuc, J.W., Menachery, V.D., Shi, P.Y., 2020. An infectious cDNA clone of SARS-CoV-2. Cell Host Microbe 27, 841–848 e843.
Xu, R., Shi, M., Li, J., Song, P., Li, N., 2020. Construction of SARS-CoV-2 virus-like particles by mammalian expression system. Front. Bioeng. Biotechnol. 8, 862.
Zhang, H., Fischer, D.K., Shuda, M., Moore, P.S., Gao, S.J., Ambrose, Z., Guo, H., 2022. Construction and characterization of two SARS-CoV-2 minigenome replicon systems. J. Med. Virol. 94, 2438–2452.
Zhang, Q.Y., Deng, C.L., Liu, J., Li, J.Q., Zhang, H.Q., Li, N., Zhang, Y.N., Li, X.D., Zhang, B., Xu, Y., Ye, H.Q., 2021a. SARS-CoV-2 replicon for high-throughput antiviral screening. J. Gen. Virol. 102, 1583.
Zhang, Y., Song, W., Chen, S., Yuan, Z., Yi, Z., 2021b. A bacterial artificial chromosome (BAC)-vectored noninfectious replicon of SARS-CoV-2. Antivir. Res. 185, 104974.
Zhou, P., Yang, X.L., Wang, X.G., Hu, B., Zhang, L., Zhang, W., Si, H.R., Zhu, Y., Li, B., Huang, C.L., Chen, H.D., Chen, J., Luo, Y., Guo, H., Jiang, R.D., Liu, M.Q., Chen, Y., Shen, X.R., Wang, X., Zheng, X.S., Zhao, K., Chen, Q.J., Deng, F., Liu, L.L., Yan, B., Zhan, F.X., Wang, Y.Y., Xiao, G.F., Shi, Z.L., 2020. A pneumonia outbreak associated with a new coronavirus of probable bat origin. Nature 579, 270–273.